Ligand Bite Governs Enantioselectivity: Electronic and Steric Control in Pd-Catalyzed Allylic Alkylations by Modular Fenchyl Phosphinites (FENOPs)**

Bernd Goldfuss,*[a] Thomas Löschmann,[b] and Frank Rominger[c]

Abstract: Modular fenchyl phosphinites (FENOPs) containing different aryl units—phenyl (**1**), 2-anisyl (**2**), or 2-pyridyl (**3**)—are efficiently accessible from (−)-fenchone. For comparison of the influence of the different aryl units on enantioselectivities and reactivities, these FENOPs were employed in Pd-catalyzed allylic alkylations. The strongly chelating character of P,N-bidentate **3** is apparent from X-ray structures with $PdCl_2$ ([Pd(**3**)Cl_2]), and with allyl–Pd units in ([Pd(**3**)(η^1-allyl)] and [Pd(**3**)(η^3-allyl)]). FENOP3 gives rise to a PdL* catalyst of moderate enantioselectivity (42% *ee*, *R* product). Surprisingly, higher enantioselectivities are found for the hemilabile, monodentate FENOPs **1** (83% *ee*, *S* enantiomer) and **2** (69% *ee*, *S* enantiomer). Only small amounts of **1** or **2** generate selective PdL* catalysts, while complete abolition of enantioselectivity appears with unselective PdL^*_2 species with higher FENOP concentrations in the cases of **1** or **2**. Computational transition structure analyses reveal steric and electronic origins of enantioselectivities. The nucleophile is electronically guided *trans* to phosphorus. *endo*-Allyl arrangements are favored over *exo*-allyl orientations for **1** and **2** due to Pd–π–pyridyl interactions with short "side-on" Pd-aryl interactions. More remote "edge-on" Pd–π–aryl interactions in **3** with Pd-N(lp) coordination favor *endo*-allyl units slightly more and explain the switch of enantioselectivity from **1** (*S*) and **2** (*S*) to **3** (*R*).

Keywords: asymmetric allylic alkylation · asymmetric catalysis · fencholates · palladium · phosphinites · transition structures

Introduction

Enantioselective, palladium-catalyzed allylic alkylations are highly valuable tools for stereoselective syntheses.[1] Three models for the design of highly selective catalysts for allylic substitutions have proven most successful:[2] "side arm guidance" of nucleophiles,[3] "chiral pockets" generated by Trost's C_2-symmetric diphosphanes based on 2-(diphenylphosphino)benzoic acid (dppba),[4] and "electronic differentiation" by different donor atoms, such as in P,N ligands (e.g., phosphinooxazolines; PHOX).[5]

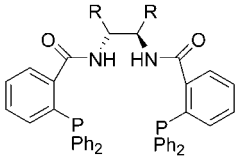

Trost ligands

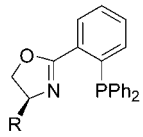

PHOX ligands

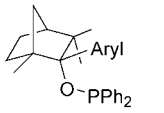

Fenchylphosphinites (FENOPs)

Phosphinooxazoline catalysts' enantioselectivities arise from electronic differentiation between coordinating P and N atoms, leading to preferential attack of nucleophiles *trans* to phosphorus.[6] In addition, enantioselectivities are also a function of steric differentiation—that is, more stable *exo* versus *endo* Pd-η^3-allylic intermediates[7]—which has been studied by X-ray analyses, NMR investigation, and quantum-chemical computations (Scheme 1).[8]

Electronic differentiation with P,N ligands is also frequently employed with pyridines.[9,10] Pyridine phosphorus ligands from chiral terpenes—such as camphor, menthone, pinocarvone, isopinocamphenol, β-pinene, and 3-carene—are well documented.[11,12,13] However, phosphorus derivatives of fenchol have been described much less frequently.[14]

[a] Prof. Dr. B. Goldfuss
Institut für Organische Chemie, Universität zu Köln
Greinstrasse 4, 50939 Köln (Germany)
Fax: (+49) 221-470-5057
E-mail: goldfuss@uni-koeln.de

[b] Dr. T. Löschmann
DSM Nutritional Products, Emil-Barell-Strasse 3
79639 Grenzach-Wyhlen (Germany)

[c] Dr. F. Rominger[+]
Organisch-Chemisches Institut
der Universität Heidelberg
Im Neuenheimer Feld 270, 69121, Heidelberg (Germany)

[+] X-ray analyses.

[**] This work is part of the Ph.D. thesis of T. L., entitled Chirale P/N-Liganden: Fenchol-Derivate für enantioselektive Katalysen, University of Heidelberg, May 2003.

DOI: 10.1002/chem.200400273

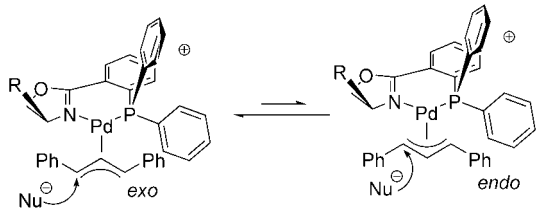

Scheme 1. Attack of nucleophiles *trans* to phosphorus in Pd-PHOX allyl complexes (R: for example, *i*Pr) as a result of electronic differentiation. Steric effects favor *exo* over *endo* allyl arrangements.

We have recently documented chelating fencholates[15] that we employed in enantioselective organozinc catalysts[16] and chiral *n*-butyllithium aggregates.[17] Here we use modular fenchyl diphenylphosphinites (FENOPs) in Pd-catalyzed allylic substitutions. Electronic and steric differentiation arises from variation of aryl units and, together with computational analyses of the transition structures, sheds light on the steric and the electronic origins of enantioselectivities.[18]

Results and Discussion

Modular fenchyl phosphinites (FENOPs) are efficiently accessible through addition of aryllithium reagents to (−)-fenchone and subsequent coupling of the fencholates with chlorophosphanes (such as Ph_2PCl). Because of their different characteristics in Pd-coordination, phenyl (**1**), 2-anisyl (**3**), and 2-pyridyl (**3**) moieties were chosen as representative aryl groups (Scheme 2).

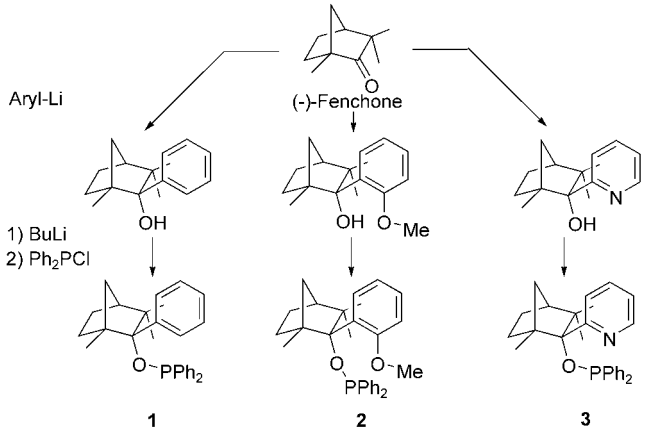

Scheme 2. Synthesis of modular fenchyl phosphinites (FENOPs).

X-ray analyses of the FENOPs **1**–**3** show that all aryls are conformationally constrained between the methyl group and the methylene bridge at C1 of the fenchane scaffolds (Figures 1, 2, and 3). Analogous rigidities had previously been

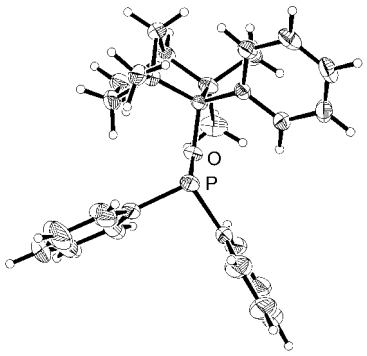

Figure 1. X-ray crystal structure of **1**. The phenyl group is fixed between the methyl group and the methylene bridge at C1 of the bicyclo[2.2.1]-heptane scaffold. The probability of the thermal ellipsoids is 50%.

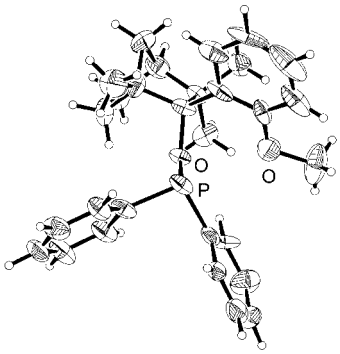

Figure 2. X-ray crystal structure of **2**. The anisyl group is fixed between the methyl group and the methylene bridge at C1 of the bicyclo[2.2.1]-heptane scaffold. The probability of the thermal ellipsoids is 50%.

Abstract in German: *Modulare Fenchylphosphinite (FENOPs) mit unterschiedlichen Arylgruppen—d.h. Phenyl (**1**), 2-Anisyl (**2**) oder 2-Pyridyl (**3**)—sind effizient aus (−)-Fenchon zugänglich. Zum Vergleich unterschiedlicher Arylgruppen hinsichtlich der erzielten Enantioselektivitäten und Reaktivitäten, wurden diese FENOPs in Pd-katalysierten allylischen Alkylierungen eingesetzt. Der stark chelatisierende Charakter des bidentaten P,N-Liganden **3** wird durch Röntgenstrukturen mit $PdCl_2$ ([Pd(**3**)Cl_2]), sowie mit Allyleinheiten ([Pd(**3**)(η^1-allyl)] und [Pd(**3**)(η^3-allyl)]) deutlich. Der bidentate P,N-Ligand **3** führt zu einem PdL* Katalysator mit moderater Enantioselektivität (42% ee, R Produkt). Überraschenderweise werden für die hemilabilen FENOP Liganden **1** (83% ee, S Enantiomer) und **2** (69% ee, S Enantiomer) höhere Enantioselektivitäten des anderen Enantiomers gefunden. Nur kleinere Mengen von **1** oder **2** bilden selektive PdL* Katalysatoren, während mit höheren FENOP Konzentrationen unselektive PdL^*_2 Spezies die Enantioselektivitäten zusammenbrechen lassen. Theoretische Berechnungen an Übergangszuständen offenbaren sterische und elektronische Ursprünge der Enantioselektivitäten. Das Nukleophil wird elektronisch kontrolliert* trans *zum P-Atom geleitet. Für **1** und **2** sind* endo- *gegenüber* exo-*Allyl Anordnungen wegen Pd–π–Pyridyl Wechselwirkungen mit kurzen "side-on" Pd-Aryl Kontakten bevorzugt. In **3** begünstigen mit ihrem größerem Abstand "edge-on" Pd–π–Aryl Wechselwirkungen durch Pd-N(lp) Koordination die* endo-*Allyl Anordnungen etwas mehr und führen so zum Wechsel des bevorzugten Enantiomers von **1** (S) und **2** (S) zu **3** (R).*

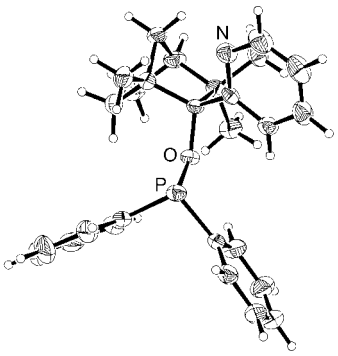

Figure 3. X-ray crystal structure of **3**. The pyridyl group is fixed between the methyl group and the methylene bridge at C1 of the bicyclo[2.2.1]-heptane scaffold. The probability of the thermal ellipsoids is 50%.

recognized in aryl fencholates employed in alkylzinc catalysts[16] or in chiral organolithium reagents.[17] The X-ray structures of palladium complexes of **3**—with chloride ([Pd(**3**)Cl_2]; Figure 4), with an η^1-allyl unit ([Pd(**3**)(η^1-allyl)]; Figure 5), and with an η^3-allyl moiety ([Pd(**3**)(η^3-allyl)]; Figure 6)—demonstrate the bidentate and chelating character of **3**. A strong *trans* influence[6] of phosphorus originating from electronic differentiation in P,N-FENOP **3** is apparent from the Pd–Cl distances in [Pd(**3**)Cl_2] (*trans* to P: 2.39 Å, versus *cis* to P: 2.28 Å; Figure 4) and from the Pd–C distances in [Pd(**3**)(η^3-allyl)] (*trans* to P: 2.25 Å versus *cis* to P: 2.16 Å; Figure 6).

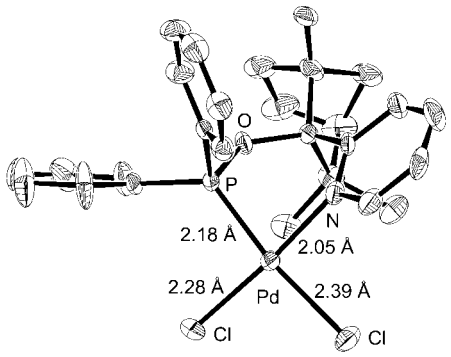

Figure 4. X-ray crystal structure of FENOP **3** with palladium chloride ([Pd(**3**)Cl_2]). Hydrogen atoms are omitted for clarity, and the probability of the thermal ellipsoids is 30%.

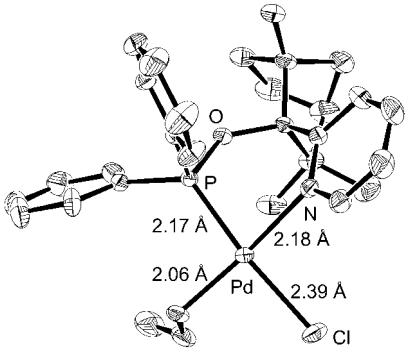

Figure 5. X-ray crystal structure of FENOP **3** with palladium η^1-allyl chloride ([Pd(**3**)(η^1-allyl)]). Hydrogen atoms are omitted for clarity, and the probability of the thermal ellipsoids is 30%.

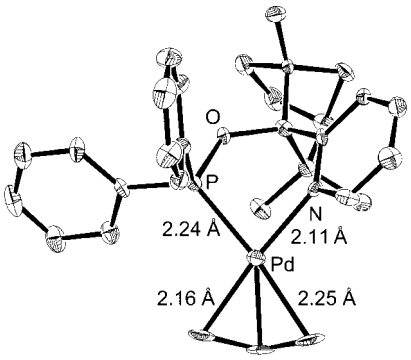

Figure 6. X-ray crystal structure of **3** with palladium η^3-allyl perchlorate ([Pd(**3**)(η^3-allyl)]). Perchlorate is not shown in the ORTEP presentation. Hydrogen atoms are omitted for clarity, and the probability of the thermal ellipsoids is 30%.

Aryl FENOPs **1**–**3** were tested in the alkylation of 1,3-diphenylallylacetate with sodium dimethylmalonate by Trost's bistrimethylsilylacetamide (BSA) procedure (Scheme 3, Table 1).[19]

Different palladium to ligand (Pd/L*) ratios were employed in the allylation of malonate to illuminate the role of catalyst compositions on enantioselectivities (Table 1, Figure 7) and on reactivities (Table 1, Figure 8). For bidentate **3**, the palladium to ligand ratio has no significant influence on the enantioselectivity, and **3** generates the *R* enantiomer with a nearly constant enantiomeric excess of 35–42% (Figure 7, Table 1). In contrast to **3**, the *S* enantiomer is favored with the phenyl and 2-anisyl FENOPs **1** and **2**. Another surprising difference with **3** is that **1** and **2** exhibit *higher* enantioselectivities with *lower* ligand loadings. The highest enantioselectivities for **1** (83% *ee*, *S*) and **2** (69% *ee*, *S*) are seen with Pd/L* ratios of 1:0.5, but enantioselectivities vanish completely for Pd/L* ratios of 1:2 (Figure 7, Table 1). Increasing the Pd/L* ratio from 1:1 to 1:2 also increases the reactivities of **1** and **2**, while the reactivity of **3** remains constant (Figure 8, Table 1).

Explanations for the similarities of **1** and **2** and their differences with **3** can be found in equilibria of palladium catalysts with the FENOP ligands (Scheme 4). The bidentate, chelating P,N-FENOP **3** has a strong tendency to form the 1:1 catalyst analogue (i.e., PdL*), as in [Pd(**3**)(η^3-allyl)] (Figure 6). In the case of **3**, a PdL* catalyst with constant selectivity and reactivity is formed at all Pd/L* ratios. In contrast, catalyst formation with the monodentate or hemilabile **1** and **2** strongly depends on the Pd/L* ratios. Larger amounts of **1** or **2** favor conformationally flexible, and

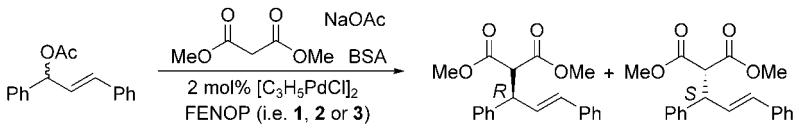

Scheme 3. Allylic alkylation of diphenylallyl acetate by sodium dimethylmalonate with catalysis by Pd-FENOP complexes.

Table 1. Pd-catalyzed allylic alkylations of diphenylallyacetate with dimethylmalonate in the presence of different Pd/FENOP ratios.[a]

Ligand	Pd/L* ratio	Chemical yield [%]	% *ee* (config.)
1	1:0.5	31	83 (*S*)
	1:1	32	81 (*S*)
	1:1.5	39	45 (*S*)
	1:2	74	0
2	1:0.5	29	69 (*S*)
	1:1	30	67 (*S*)
	1:1.5	55	55 (*S*)
	1:2	70	0
3	1:0.5	< 10	35 (*R*)
	1:1	> 99	42 (*R*)
	1:1.5	> 99	41 (*R*)
	1:2	> 99	42 (*R*)

[a] Solvent: CH_2Cl_2, 24 h, −20 °C, c.f. experimental procedure.

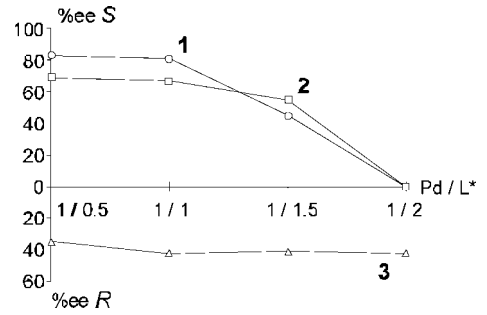

Figure 7. Enantioselectivities of Pd-FENOP-catalyzed allylations of dimethylmalonate (CH_2Cl_2, 24 h, −20 °C) with different palladium to FENOP ligand (Pd/L*) ratios.

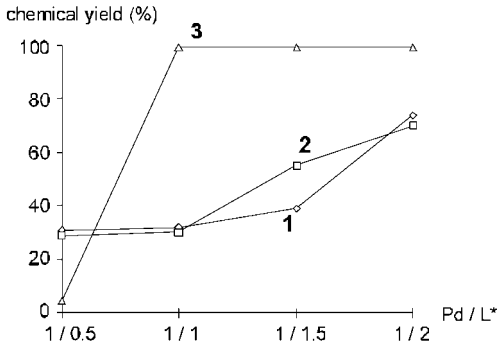

Figure 8. Chemical yields of Pd-FENOP-catalyzed allylations of dimethylmalonate (CH_2Cl_2, 24 h, −20 °C) with different palladium to FENOP-ligand (Pd/L*) ratios.

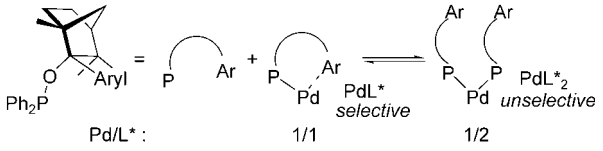

Scheme 4. Equilibrium of FENOP palladium complexes. Bidentate **3** (Ar = 2-pyridyl) forms a permanent PdL* catalyst, while monodentate **1** (Ar = phenyl) and **2** (Ar = 2-anisyl) give both selective PdL* *and* unselective PdL^*_2 complexes, depending on the FENOP concentrations.

hence unselective, 1:2 catalysts (i.e., PdL^*_2), while smaller amounts of FENOP yield the more selective, but less reactive, PdL* catalysts for **1** and **2** (Scheme 4). For one class of phosphinooxazolines, even a switch in enantioselectivity from the *S* to the *R* enantiomers with a changing Pd/L* ratio was observed, and was explained in terms of analogous equilibria.[20]

^{31}P NMR experiments with **1** and palladium allyl chloride ($[Pd(C_3H_5)Cl]_2$) also support such $PdL^* \rightleftarrows PdL^*_2$ equilibria. For large FENOP amounts—for a Pd/L* ratio of 1:2, for example—the ^{31}P signal (δ = 78.1 ppm) is consistent with a PdL^*_2 complex (Figure 9). Decreasing amounts of ligand—

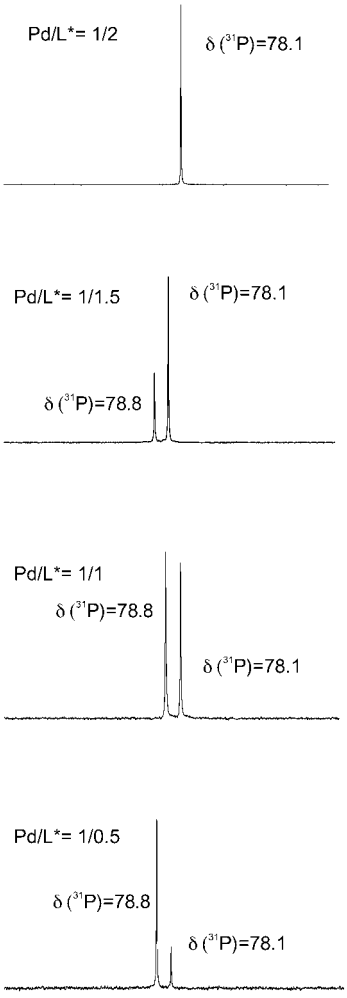

Figure 9. ^{31}P NMR spectra of FENOP **1** with $[\{Pd(C_3H_5)Cl\}_2]$ at different palladium to ligand (Pd/L*) ratios (CD_2Cl_2, 25 °C). The signals at δ = 78.1 and 78.8 ppm can be assigned to PdL^*_2 and PdL* complexes, respectively.

for Pd/L* ratios of 1:1.5, 1:1, and finally 1:0.5, for example—give rise to a new ^{31}P signal (δ = 78.8 ppm), which can be assigned to the corresponding PdL* complex. Although described as monodentate, aryl P-ligand units such as **1** and **2** are likely to form Pd–C π-contacts, as is known for, for example, the monophosphanes MOP or MAP.[21]

Computational analyses of Pd-η^3-allyl complexes have proven to be very helpful in explaining equilibria and enan-

tioselectivities for PHOX ligands by comparison with η^3-allylic intermediates.[6b,8] Thanks to the significance of Curtin–Hammett conditions,[22] assessments of transition structures for enantioselective steps are even more revealing.[23] Ammonia was used as a model to mimic the experimentally used malonate nucleophile (the suitability of NH_3 as a model nucleophile in Pd-catalyzed allylic substitutions was demonstrated recently[23]) for such computational ONIOM-(B3LYP:UFF) transition structure analyses with the FENOPs **1**, **2**, and **3**. As is apparent from selectivity (Figure 7) and reactivity (Figure 8) studies, the enantioselective FENOP catalysts have PdL* compositions. The four transition structures of PdL* η^3-allylic complexes differ in the *exo* and *endo* alignments of the allyl moieties as well as in the *trans* or *cis* attack of the nucleophile relative to phosphorus (Scheme 5, Table 2).[24]

Transition structures of **1** and **2** favor *endo*-aligned allyl units with attack of the nucleophile *trans* to phosphorus (Table 2), yielding *S* enantiomeric products, in agreement with experimental results (Table 1).[23] In contrast, bidentate FENOP **3** slightly favors an *exo*-aligned allyl moiety (Table 2), again with attack of the nucleophile *trans* to phosphorus, producing the *R* enantiomer, as observed experimentally (Table 1).[23]

This kinetic preference for attack *trans* to phosphorus in the transition structures of the FENOPs is consistent with longer (and weaker) allylic Pd–$C_{(trans\ P)}$ bonds, frequently observed in η^3-allyl Pd complexes,[6,8,20a] as in [Pd(**3**)(η^3-allyl)] (Figure 6). Such a kinetic *trans* phosphane preference is also apparent from transition structures of nucleophilic additions of NH_3 to the smaller model complex [Pd(η^3-allyl)(pyridine)(PH_3)]$^+$ (Figure 10). The higher reactivity of the *trans* (to P) allylic position is apparent from a longer H_3N–C_{allyl} (2.007 Å) and a shorter Pd–C_{allyl} distance (2.787 Å) relative to the *cis* transition structure (1.939 and 2.784 Å respectively, Figure 10). Hence, the more reactive *trans* attack is earlier on the reaction coordinate than the *cis* addition, in accordance with the Hammond postulate.[25] Phosphane, as the better (σ*) acceptor, stabilizes the developing Pd-nucleofuge of this S_N2(C) step in a *trans* position better than it does in a *cis* site. Consistently, phosphane avoids the *trans* arrangement relative to more electrophilic allylic positions.[6b] Although **1** and **2** were expected to be monodentate, the transition structures with **1** and **2** have rather short Pd–C–π contacts

Table 2. Transition structures of phenyl (**1**), 2-anisyl (**2**), and 2-pyridyl (**3**) FENOP-Pd-diphenylallyl complexes with NH_3.[a]

	Comput.	*exo-trans* (***R***)	*endo-trans* (***S***)	*exo-cis* (***S***)	*endo-cis* (***R***)
1	TS	−651.20519	−651.21001	−651.20660	−651.20488
	ZPE, Freq	525.7, *i*148	525.7, *i*159	525.7, *i*175	525.7, *i*170
	E_{rel}	+3.0	**0.0**	+2.1	+3.2
2	TS	−765.10237	−765.10785	−765.10039	−765.09965
	ZPE, Freq	546.3, *i*161	546.2, *i*163	546.5, *i*172	546.0, *i*172
	E_{rel}	+3.5	**0.0**	+5.0	+4.9
3	TS	−667.15780	−667.15767	−667.14917	−667.15472
	ZPE, Freq	518.1, *i*148	518.3, *i*153	518.4, *i*168	518.4, *i*184
	E_{rel}	**0.0**	+0.3	+5.7	+2.2

[a] ONIOM (B3LYP/LanL2DZ (Pd, P), 3–21G (C, H, N, O): UFF) extrapolated total energies of optimized structures [a.u.]. The imaginary (*i*) frequencies [cm^{-1}] correspond to the allylic substitution step (C–N bond-formation) with NH_3 as model nucleophile.[23] Zero-point energies [kcal mol^{-1}] were unscaled considered for relative energies E_{rel} [kcal mol^{-1}].

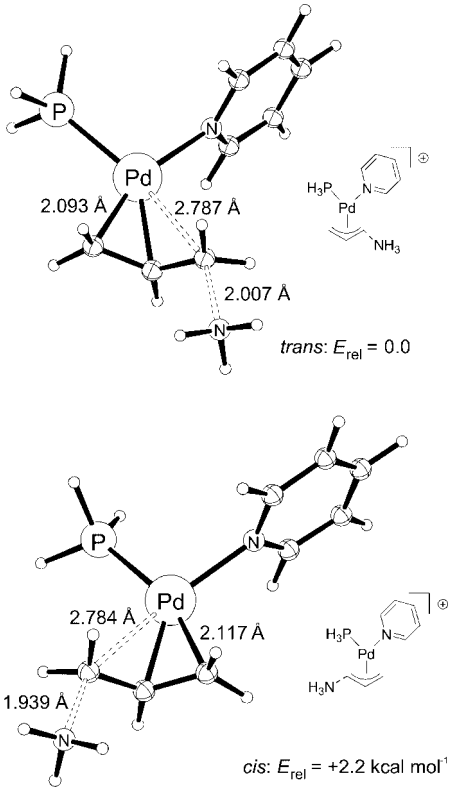

Figure 10. B3LYP/LanL2DZ(ECP)+d,p (Pd, P)/6–31G*(C,H)/6–31+G*(N) optimized transition structures of the nucleophilic NH_3 addition to [Pd(η^3-allyl)(pyridine)(PH_3)]$^+$. *trans*: −557.04144 a.u., ZPE: 142.9 kcal mol^{-1}, *i*230 cm^{-1}, E_{rel}: 0.0; *cis*: −557.03801 a.u., ZPE: 143.0 kcal mol^{-1}, *i*278 cm^{-1}, E_{rel}: + 2.2 kcal mol^{-1}.

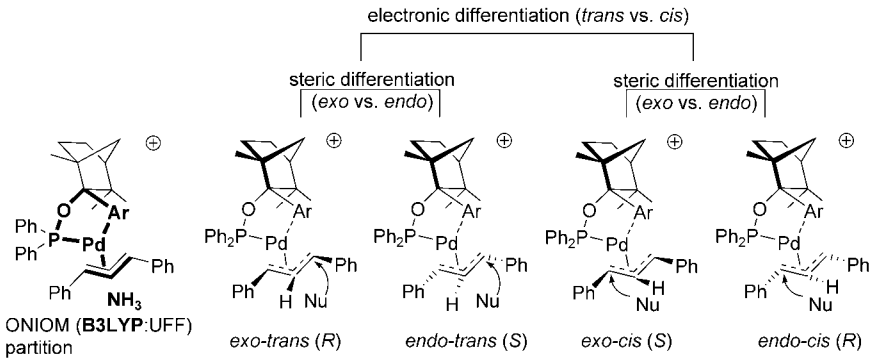

Scheme 5. Optimized ONIOM (B3LYP (partition in bold):UFF) transition structures (Nu = NH_3) for Pd-FENOP-catalyzed allylic substitutions with *exo* or *endo* alignments of diphenylallyl groups and *trans* or *cis* attack of the nucleophile relative to phosphorus, yielding *S* or *R* enantiomers.[23]

(Figure 11 and 12). This Pd–C π bonding contributes to electronic differentiation in **1** and **2** and is also observed in Pd–aryl monophosphane complexes.[21]

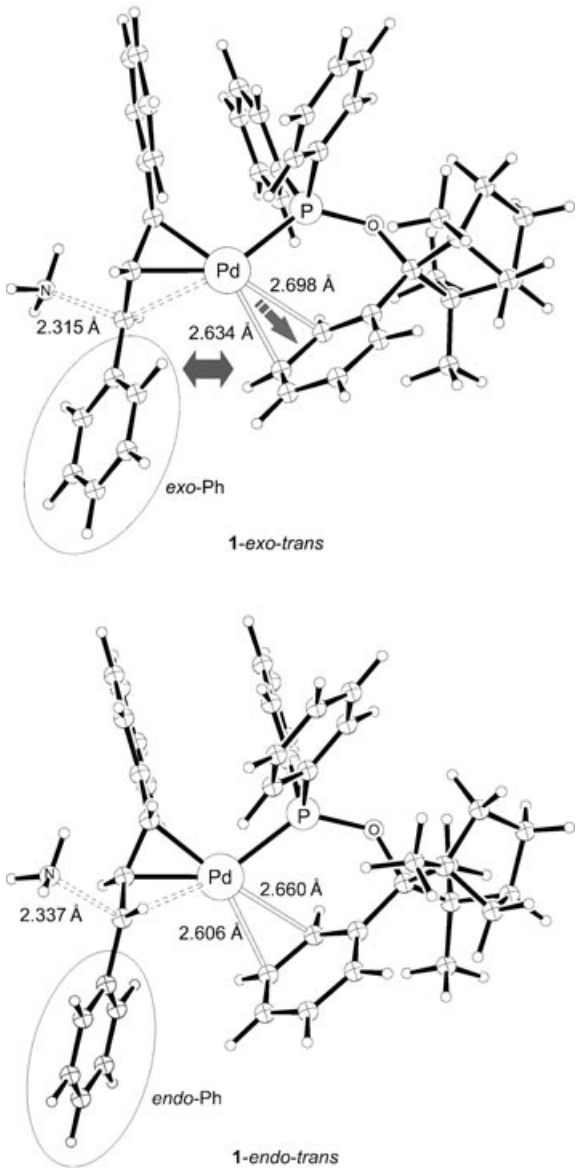

Figure 11. ONIOM(B3LYP/LanL2DZ(ECP) (Pd, P)/3–21G (C, O, N, H): UFF) optimized transition structures. The higher stability (3.0 kcal mol^{-1}) of **1**-*endo-trans* is due to better Pd–Ph π-interaction than in **1**-*exo-trans*, which is hindered by its *exo*-phenyl group.

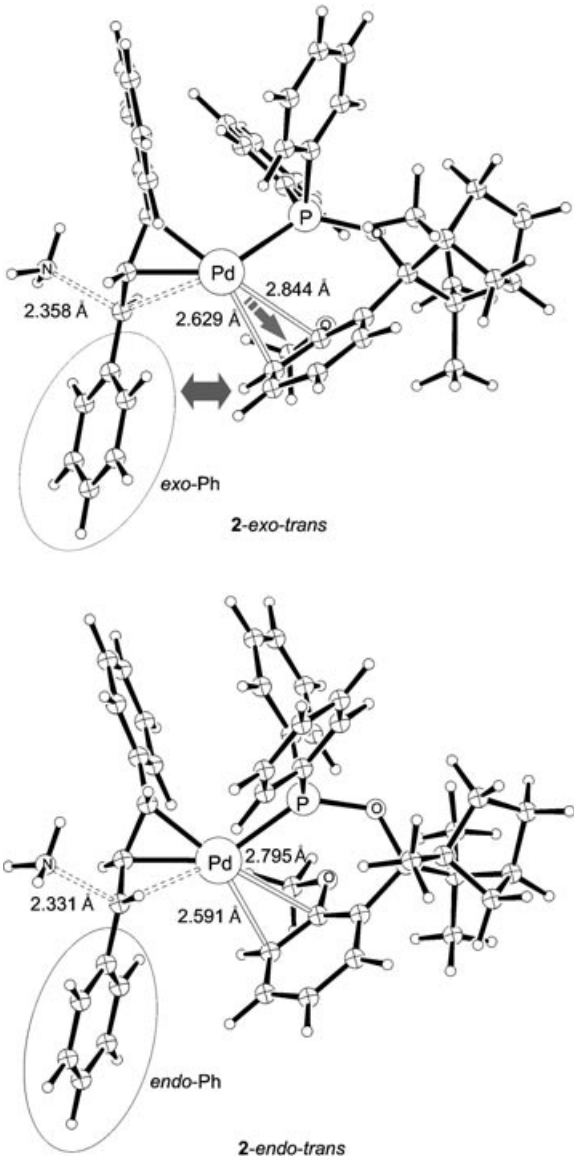

Figure 12. ONIOM(B3LYP/LanL2DZ(ECP) (Pd, P)/3–21G (C, O, N, H): UFF) optimized transition structures. The higher stability (3.5 kcal mol^{-1}) of **2**-*endo-trans* is due to better Pd–Ph π-interaction than in **2**-*exo-trans*, which is hindered by its *exo*-phenyl group.

In addition to electronic differentiation, the steric bias between *exo*- and *endo*-aligned allyl moieties is crucial for enantioselectivities. The *S* enantiomer obtained from **1** and **2** originates from most stable *endo-trans* transition structures, which are favored over the *exo-trans* alignments for steric reasons, as both exhibit attack *trans* to P (Table 2). In *exo-trans* structures, allylic phenyl groups point to *exo*-hemispheres and come close to the axial Ph–P(Ph) units as well as to the aryl groups, which π-coordinate to Pd. This π-coordination is hence significantly hindered in the *exo* transition structures, but not in the *endo-trans* transition structures with *endo*-oriented allyl-phenyl groups. As a consequence, Pd–C π-contacts in the favored *endo* structures are significantly shorter than in the hindered *exo* structures (Figure 11 and 12). This steric preference, together with electronically favored *trans*-(P)-addition, explains the origin of enantioselectivity for **1** and **2**.

The switch of enantioselectivity from **1** and **2** (*S* enantiomer) to **3** (*R* enantiomer, Table 1) can be explained in terms of different coordination modes of the FENOP aryls. The bias of the *exo-trans* transition structures of **1** (Figure 11) and **2** (Figure 12) due to hindrance of π-aryl "side-on" coordination to Pd does not appear for **3**, which shows N-lone pair "edge-on" coordination of the pyridine unit to Pd (Figure 13). This N–Pd contact results in a more remote pyridyl moiety, which is hence less repulsive for *exo*-allylic phenyl groups. The N–Pd coordination also bends the

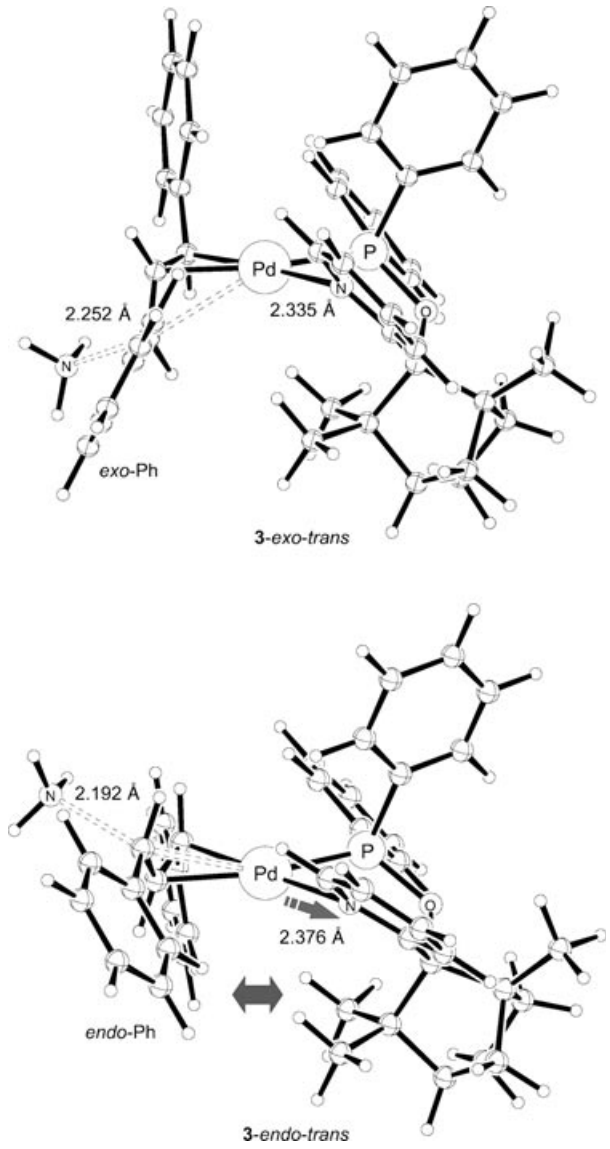

Figure 13. ONIOM(B3LYP/LanL2DZ(ECP) (Pd, P)/3-21G (C, O, N, H): UFF) optimized transition structures. The slightly higher stability (0.3 kcal mol^{-1}) of **3**-*exo-trans* can be explained in terms of less repulsive *endo*-fenchane interactions relative to **3**-*endo-trans*.

ligand on the *endo*-hemisphere more to the allylic substrate (Figure 13) and *endo*-allylic phenyl groups hence become less favorable for **3**. This explains the slight preference of **3** for the *R* enantiomer, while **1** and **2** yield *S* products (Table 1).

The origins of the different enantioselectivities with **1**, **2**, and **3** can hence be explained in terms of electronic and steric effects, computed in transition structures with PdL* compositions. Chelate formation, either through π-aryl coordination to Pd as in **1** and **2** or through the N-lp coordination to Pd as in **3**, is crucial for the enantioselectivities. Complete abolition of enantioselectivity arises for the hemilabile FENOPs **1** and **2**, apparently due to high conformational flexibility, with higher ligand loadings and formation of catalysts with PdL*$_2$ composition.

Conclusions

Applications of modular fenchyl phosphinites (FENOPs) with different aryl units—phenyl (**1**), 2-anisyl (**2**), or 2-pyridyl (**3**)—in Pd-catalyzed allylic substitutions show how electronic and steric effects of aryl groups on enantioselectivities can be differentiated. Strongly chelating **3** gives a PdL* catalyst with moderate enantioselectivity (42 % *ee*, *R* product), while hemilabile **1** (83 % *ee*, *S*) and **2** (69 % *ee*, *S*), yield higher enantioselectivities, but only if small amounts of FENOP are employed. The annihilation of enantioselectivity at higher FENOP concentrations, suggesting flexible and unselective PdL*$_2$ catalysts, demonstrates the crucial role of well defined and rigid chelate structures. Consistently with previous results and suggestions, nucleophiles guided *trans* to phosphorus are preferred electronically. Sterically, *endo* or exo arrangements of allylic alkyl groups give rise to repulsive interactions with the ligand moiety. Hence, it is likely that less demanding groups, such as dimethylallyl, should give lower enantioselectivities. "Edge-on" pyridine coordination in **3** vs. "side on" π-aryl coordination in **1** and **2**, results in a switch of enantioselectivity from *R* (**3**) to *S* products (**1** and **2**). This π-aryl coordination of **1** and **2** can play a crucial role in controlling enantioselectivity not only through steric effects but also through electronic P,π-aryl-differentiation, as is established for P,N ligands. Together with steric effects, electronic P,π–aryl differentiation might become an efficient tool for the design of catalysts in various kinds of reactions open to electronic differentiation.

Experimental Section

General: The reactions were carried out under argon atmosphere (Schlenk and needle/septum techniques) with dried and degassed solvents. X-ray crystal analyses were performed on a Bruker Smart CCD diffractometer with use of $Mo_{K\alpha}$ radiation, NMR spectra were recorded on a Bruker AMX 300 instrument, IR spectra on a Bruker Equinox 55 FT-IR spectrometer, and optical rotations on a Perkin Elmer P241 machine. GC analyses were carried out on a Chrompack (CP9001) instrument.

CCDC-232671–232676 contains the supplementary crystallographic data for this paper. These data can be obtained free of charge via www.ccdc.cam.ac.uk/conts/retrieving.html (or from the Cambridge Crystallographic Data Centre, 12, Union Road, Cambridge CB2 1EZ, UK; fax: (+44) 1223-336-033; or deposit@ccdc.cam.ac.uk).

Synthesis of diphenyl-((1*R*,2*R*,4*S*)-1,3,3-trimethyl-2-phenylbicyclo[2.2.1]-hept-2-yl)-phosphinite (1): Phenylfenchol was synthesized by addition of phenyllithium to (−)-fenchone and hydrolytic workup.[26] This phenylfenchol (5.16 g, 0.022 mol) was dissolved in THF (100 mL), the mixture was cooled to 0 °C, and *n*-butyllithium in hexanes (1.6 M, 0.022 mol) was added. Use of an excess of *n*-butyllithium, apparent from a change from yellow to orange, should be avoided due to unfavorable side products. Freshly distilled chlorodiphenyl phosphane (0.022 mol) was added to this cooled solution, and the reaction mixture was allowed to warm to room temperature and stirred for two days. The solvent and volatile components were removed in vacuum under inert gas conditions, and the obtained yellow oil was dissolved in toluene. Lithium chloride was removed by filtration over celite, and toluene was removed in vacuum. The yellow oil was dissolved in diethyl ether and cooled to −20 °C. The resulting white precipitate was washed with cold (−20 °C) pentane and dried in vacuum. Yield: 6.47 g (71 %).

Analytic and spectroscopic data for 1: m.p. 127–130 °C; $[\alpha]_{Na}^{21} = -99.6$; ^{1}H NMR ($CDCl_3$, 300 MHz): Δ = 0.51 (s, 3H; CH_3), 0.75 (m, 1H; 6-

exo), 1.15–1.25 (m, 2H; 7-*anti*, 5-*exo*), 1.30 (s, 3H; CH_3), 1.45 (s, 3H; CH_3), 1.65–1.8 (m, 3H; CH, 5-*endo*, 7-*syn*), 2.35 (m, 1H; 6-*endo*), 7.0–7.7 ppm (m, 15H_{ar}); $^{13}C\{^1H,^{31}P\}$ NMR ($CDCl_3$, 75.5 MHz): Δ = 18.9 (CH_3), 21.5 (CH_3), 24.1 (CH_2), 32.6 (CH_3), 33.9 (CH_2), 37.9 (CH_2), 46.1 (CH_q), 48.9 (CH), 52.6 (CH_q), 104.9 (CH_q), 125.7 (C_{ar}), 126.0 (C_{ar}), 126.8 (C_{ar}), 127.8 ($C_{ar/q}$), 128.1 ($C_{ar/q}$), 128.6 (C_{ar}), 128.8 ($C_{ar/q}$), 129.2 (C_{ar}), 130.5 (C_{ar}), 131.3 (C_{ar}), 132.3 (C_{ar}), 132.8 ppm (C_{ar}); $^{31}P\{^1H\}$ NMR ($CDCl_3$, 121.5 MHz): Δ = 88.8 ppm (s); IR (KBr): $\tilde{\nu}$ = 3054, 3014 (C_{ar}–H, w), 2928 (C_{alk}–H, m) cm^{-1}; MS (FAB): *m/z* (%): 414.2 $[M]^+$, 213.2 $[M-OPPh_2]^+$; elemental analysis calcd (%) for $C_{28}H_{31}OP$ (414.52 $g\,mol^{-1}$): C 81.12, H 7.54, P 7.48; found: C 81.11, H 7.53, P 7.27.

X-ray crystal data for 1: $C_{28}H_{31}OP$; M_r = 414.50; space group $P2_1/c$; monoclinic; *a* = 20.1083(3), *b* = 12.2746(1), *c* = 9.3068(1) Å, β = 96.446(1)°; *V* = 2282.59(5) $Å^3$; *Z* = 4; *T* = 200(2) K; μ = 0.137 mm^{-1}; reflections total: 23178, unique: 5214, observed: 4297 ($I>2\sigma(I)$); *R*1 = 0.041, *wR*2 = 0.104; GOF = 1.04.

Synthesis of 2-(2-methoxyphenyl)-1,3,3-trimethylbicyclo[2.2.1]hept-2-yl-diphenylphosphinite (2): 2-Methoxyfenchol was synthesized by addition of anisyllithium to (−)-fenchone and hydrolytic workup.[16e,17b] This 2-methoxyfenchol (6.30 g, 0.024 mol) was dissolved in THF (100 mL), the mixture was cooled to 0°C, and *n*-butyllithium in hexanes (1.6 M, 0.022 mol) was added. Further reaction and workup and removal of lithium chloride were performed analogously to the synthesis of **1**. The resulting yellow oil was diluted with acetone (3 mL) and stirred at room temperature. The obtained colorless precipitate was washed with cold (−20°C) acetone, recrystallized from diethyl ether, and dried in vacuum. Yield: 6.93 g (65%).

Analytic and spectroscopic data for 2: m.p. 103–104°C; $[\alpha]_{Na}^{21}$ = −45.3; ^1H NMR ($CDCl_3$): Δ = 0.45 (s, 3H; CH_3), 1.05 (m, 1H; 6-*exo*), 1.15–1.2 (m, 2H; 7-*anti*, 5-*exo*), 1.20 (s, 3H; CH_3), 1.39 (s, 3H; CH_3), 1.75–1.85 (m, 3H; CH, 5-*endo*, 7-*syn*), 2.25 (m, 1H; 6-*endo*), 2.9 (s, 3H; OCH_3), 6.9–7.65 ppm (m, 14H_{ar}); $^{13}C\{^1H,^{31}P\}$ NMR ($CDCl_3$): δ = 19.4 (CH_3), 24.2 (CH_3), 24.9 (CH_2), 29.0 (CH_3), 34.3 (CH_2), 41.9 (CH_2), 46.9 (CH_q), 50.4 (CH), 53.2 (OCH_3), 53.3 (CH_q), 94.5 (CH_q), 109.8 (C_{ar}), 118.5 (C_{ar}), 127.4 (C_{ar}), 127.6 (C_{ar}), 127.8 (C_{ar}), 129.0 (C_{ar}), 129.3 (C_{ar}), 129.7 (C_{ar}), 130.2 (C_{ar}), 132.8 (C_{ar}), 144.6 (C_{ar}), 146.6 (C_{ar}), 155.9 (C_{ar}), 158.7 ppm (C_{ar}); $^{31}P\{^1H\}$ NMR ($CDCl_3$): Δ = 89.6 ppm (s); IR (KBr): $\tilde{\nu}$ = 3057 (C_{ar}–H, w), 2984–2876 (C_{alk}–H, m) cm^{-1}; MS (FAB): *m/z* (%): 444.3 $[M]^+$, 413.3 $[M-OMe]^+$; elemental analysis calcd (%) for $C_{29}H_{33}O_2P$ (444.54 $g\,mol^{-1}$): C 78.35, H 7.48, P 6.97; found: C 78.18, H 7.53, P 6.82.

X-ray crystal data for 2: $C_{29}H_{33}O_2P$; M_r = 444.52; space group $P2_1$; monoclinic; *a* = 8.2728(1), *b* = 11.6341(2), *c* = 25.4731(4) Å, β = 93.283(1); *V* = 2447.67(6) $Å^3$; *Z* = 4; *T* = 200(2) K; μ = 0.135 mm^{-1}; reflections total: 15634, unique: 5794, observed: 4995 ($I>2\sigma(I)$); *R1* = 0.080, *wR*2 = 0.211; GOF = 1.16.

Synthesis of diphenyl-((1*R*,2*R*,4*S*)-1,3,3-trimethyl-2-pyridin-2-ylbicyclo[2.2.1]hept-2-yl)phosphinite (3): 2-Pyridinylfenchol was synthesized by lithiation of 2-bromopyridine, subsequent addition to (−)-fenchone, and hydrolytic workup.[27] Pyridinylfenchol (10.0 g, 0.043 mol) was dissolved in THF (100 mL), the mixture was cooled to 0°C, and *n*-butyllithium in hexanes (1.6 M, 0.022 mol) was added. Further reaction and workup and removal of lithium chloride were performed analogously to the synthesis of **1**. The resulting yellow oil was diluted with diethyl ether (3 mL) and stirred at room temperature. The obtained colorless precipitate was washed with cold (−20°C) pentane and dried in vacuum. Yield: 15.8 g (88%).

Analytical and spectroscopic data for 3: m.p. 122–123°C; $[\alpha]_{Na}^{21}$ = −93.5; ^1H NMR ($CDCl_3$): Δ = 0.37 (s, 3H; CH_3), 0.72–0.79 (m, 1H; 6-*exo*), 1.17 (m, 1H; 7-*anti*), 1.36 (m, 4H; 5-*exo*, CH_3), 1.5 (s, 3H; CH_3), 1.65–1.90 (m, 3H; CH, 5-*endo*, 7-*syn*), 2.76 (m, 1H; 6-*endo*), 7.0 (m, 1H_{ar}), 7.2 (m, 1H_{ar}), 7.3–7.45 (m, 7H_{ar}), 7.55–7.75 (m, 4H_{ar}), 8.5 ppm (m, 1H_{ar}); $^{13}C\{^1H,^{31}P\}$ NMR ($CDCl_3$): δ = 18.4 (CH_3), 22.9 (CH_3), 24.9 (CH_2), 29.2 (CH_3), 32.8 (CH_2), 43.0 (CH_2), 48.5 (C_q), 48.8 (CH), 53.9 (C_q), 94.2 (C_q), 121.1 (C_{ar}), 124.2 (C_{ar}), 128.2 (C_{ar}), 128.4 (C_{ar}), 129.1 (C_{ar}), 129.3 (C_{ar}), 131.5 (C_{ar}), 131.7 (C_{ar}), 134.7 (C_{ar}), 143.2 (C_{ar}), 145.2 (C_{ar}), 147.1 (C_{ar}), 163.0 ppm ($C_{ar/q}$); $^{31}P\{^1H\}$ NMR ($CDCl_3$): δ = 90.8 ppm (s); IR (KBr): $\tilde{\nu}$ = 3070 (C_{ar}–H, w), 2994–2890 (C_{alk}–H, m) cm^{-1}; MS (FAB): *m/z* (%): 415.5 $[M]^+$; elemental analysis calcd (%) for $C_{27}H_{30}NOP$ (415.51 $g\,mol^{-1}$): C 78.05, H 7.28, N 3.37, P 7.45; found: C 77.80, H 7.16, N 3.42, P 7.43.

X-ray crystal data of 3: (21% oxidized to the PO derivative) $C_{27}H_{30}NOP$; M_r = 415.49; space group $P2_12_12_1$; orthorhombic; *a* = 8.9718(1), *b* = 14.0985(1), *c* = 18.1265(2) Å, β = 93.283(1); *V* = 2292.80(4) $Å^3$; *Z* = 4; *T* = 200(2) K; μ = 0.138 mm^{-1}; reflections total: 23918, unique: 5254, observed: 4270 ($I>2\sigma(I)$); *R*1 = 0.039, *wR*2 = 0.081; GOF = 1.01.

Synthesis and characterization of palladium complexes with [Pd(3)Cl$_2$]: FENOP **3** (41.6 mg, 0.1 mmol) and $[PdCl_2(CH_3CN)_2]$ (25.9 mg, 0.1 mmol) were dissolved in CH_2Cl_2 (2 mL). The mixture was stirred for 1 h at room temperature. Slow evaporation of the solvent (U-Schlenk tube) yielded crystals suitable for X-ray analysis. M.p. 185°C (decomp); $^{31}P\{^1H\}$ NMR (CD_2Cl_2, 121.5 MHz): Δ = 80.0 ppm (s).

X-ray crystal data for [Pd(3)Cl$_2$]: $C_{27}H_{30}Cl_2NOPPd$; M_r = 592.83; space group $P6_3$; hexagonal; *a* = 20.9745(1), *b* = 20.9745(1), *c* = 13.0226(2) Å; *V* = 4961.48(8) $Å^3$; *Z* = 6; *T* = 200(2) K; μ = 0.793 mm^{-1}; reflections total: 36892, unique: 4769, observed: 3895 ($I>2\sigma(I)$); *R*1 = 0.048, *wR*2 = 0.128; GOF = 1.07.

[Pd(3)(η^1-allyl)]: FENOP **3** (41.6 mg, 0.1 mmol) and $[\{PdCl(C_3H_5)\}_2]$ (18.3 mg, 0.05 mmol) were dissolved in CH_2Cl_2 (1 mL). The mixture was stirred for 1 h at room temperature. Slow evaporation of the solvent (U-Schlenk tube) yielded crystals suitable for X-ray analysis. M.p.: 170°C (decomposition). In solution, η^3-*endo*/*exo* isomers (A/B) could be identified with a ratio of A/B = 0.8:1 at 233 K. *endo*/*exo*-isomer A: ^1H NMR (CD_2Cl_2): Δ = 0.61 (s, 3H), 1.34 (s, 3H), 1.38 (s, 3H), 1.49 (m, 4H), 1.83 (d, 1H), 2.31 (d, 1H), 2.43 (m, 1H), 2.97 (d, 1H_{allyl}), 4.08 (dd, 1H_{allyl}), 4.16 (dd, 1H_{allyl}), 4.83 (t, 1H_{allyl}), 6.10 (m, 1H_{allyl}), 7.1–8.1 (m, 13H; H_{ar}), 8.9 ppm (d, 1H; H_{ar}); $^{31}P\{^1H\}$ NMR (CD_2Cl_2): Δ = 117.2 ppm (s). *endo*/*exo*-isomer B: ^1H NMR (CD_2Cl_2): Δ = 0.50 (s, 3H), 1.19 (s, 3H), 1.28 (s, 3H), 1.49 (m, 3H), 1.67 (m, 1H), 1.83 (d, 1H), 2.25 (d, 1H), 2.57 (m, 1H), 3.54 (d, 1H_{allyl}), 3.76 (d, 1H_{allyl}), 4.00 (dd, 1H_{allyl}), 4.88 (t, 1H_{allyl}), 5.78 (m, 1H_{allyl}), 7.1–8.1 (m, 13H; H_{ar}), 9.14 ppm (d, 1H; H_{ar}); $^{31}P\{^1H\}$ NMR (CD_2Cl_2): Δ = 116.7 ppm (s). *exo*/*endo* isomers quickly equilibrate at room temperature, averaged signals appear: $^{13}C\{^1H,^{31}P\}$ NMR (CD_2Cl_2): Δ = 19.2 (CH_3), 23.9 (CH_2), 24.6 (CH_3), 28.8 (CH_3), 34.1 (CH_2), 40.0 ($CH_{2/allyl\text{-}cis\text{-}P}$), 41.7 ($CH_2$), 46.7 ($C_q$), 50.2 (CH), 53.1 ($C_q$), 93.9 ($C_q$), 98.2 ($CH_{2/allyl\text{-}trans\text{-}P}$), 109.6 ($C_{ar}$), 118.3 ($C_{ar}$), 127.1 ($C_{ar/q}$), 127.3 ($C_{ar/q}$), 127.7 ($C_{ar}$), 134.5 ($CH_{allyl\text{-}central}$), 128.8 ($C_{ar}$), 129.1 ($C_{ar}$), 129.4 ($C_{ar}$), 130.0 ($C_{ar}$), 132.4 ($C_{ar}$), 143.7 ($C_{ar}$), 146.3 ($C_{ar}$), 158.4 ($C_{ar/q}$) ppm.

X-ray crystal data for [Pd(3)(η^1-allyl)]: $C_{32}H_{39}Cl_5NOPPd$; M_r = 768.26; space group $P2_1$; monoclinic; *a* = 10.0562(1), *b* = 17.5530(2), *c* = 10.6376(2) Å, β = 110.482(1)°; *V* = 1759.01(4) $Å^3$; *Z* = 2; *T* = 200(2) K; μ = 0.978 mm^{-1}; reflections total: 18268, unique: 8055, observed: 7400 ($I>2\sigma(I)$); *R*1 = 0.031, *wR*2 = 0.079; GOF = 1.03.

[Pd(3)(η^3-allyl)]: FENOP **3** (41.6 mg, 0.1 mmol) and $[PdCl(C_3H_5)]_2$ (18.3 mg, 0.05 mmol) were dissolved in acetone (1 mL). The mixture was stirred for 1 h at room temperature. Lithium perchlorate (80.3 mg, 0.5 mmol) in acetone (1 mL) was added to this solution. After the mixture had been stirred for 30 min., water (ca. 3 mL) was added until no further precipitate was formed. Drying of the precipitate and recrystallization from diethyl ether/acetone yielded crystals suitable for X-ray analysis. M.p. 165°C (decomp).

^1H NMR (CD_2Cl_2): Δ = 0.52 (s, 3H; CH_3); 1.25 (s, 3H; CH_3); 1.36–1.43 (m, 1H; 6-*exo;* m, 1H; 7-*anti;* m, 1H; 5-*exo*); 1.83 (s, 3H; CH_3); 1.92 (m, 1H; CH; m, 1H; 5-*endo*), 2.11 (m, 1H; 7-*syn*), 2.29 (m, 1H; H_{allyl}), 2.60–2.70 (m, 1H; 6-*endo*; m, 1H; H_{allyl}); 4.08 (m, 1H; H_{allyl}), 4.38 (m, 1H; H_{allyl}), 5.95 (m, 1H; H_{allyl}), 7.00–7.70 (m, 14H; H_{ar}), 9.38 (m, 1H; H_{ar}) ppm; $^{13}C\{^1H,^{31}P\}$ NMR (CD_2Cl_2): Δ = 19.2 (CH_3), 23.9 (CH_2), 24.6 (CH_3), 28.8 (CH_3), 34.1 (CH_2), 40.0 ($CH_{2/allyl\text{-}cis\text{-}P}$) 41.7 ($CH_2$), 46.7 ($C_q$), 50.2 (CH), 53.1 ($C_q$), 93.9 ($C_q$), 98.2 ($CH_{2/allyl\text{-}trans\text{-}P}$), 109.6 ($C_{ar}$), 118.3 ($C_{ar}$), 127.1 ($C_{ar}$), 127.3 ($C_{ar/q}$), 127.7 ($C_{ar/q}$), 134.5 ($CH_{allyl\text{-}central}$), 128.8 ($C_{ar}$), 129.1 ($C_{ar}$), 129.4 ($C_{ar}$), 130.0 ($C_{ar}$), 132.4 ($C_{ar}$), 143.7 ($C_{ar}$), 146.3 ($C_{ar}$), 158.4 ($C_{ar/q}$) ppm; $^{31}P\{^1H\}$ NMR (CD_2Cl_2): Δ = 119.5 ppm (s).

X-ray crystal data for [Pd(3)(η^3-allyl)]: $C_{30}H_{35}ClNO_5PPd$; M_r = 662.41; space group $P2_1$; monoclinic; *a* = 10.313(4), *b* = 9.141(3), *c* = 15.543(7) Å, β = 102.40(3)°; *V* = 1431.1(9) $Å^3$; *Z* = 2; *T* = 200(2) K; μ = 0.838 mm^{-1}; reflections total: 8902, unique: 4100, observed: 3016 ($I>2\sigma(I)$); *R*1 = 0.046, *wR*2 = 0.093; GOF = 1.00.

General procedure for FENOP-Pd-catalyzed allylic substitutions: $[\{PdCl(C_3H_5)\}_2]$ (4.2 mg, 0.011 mmol) and FENOP ligand (0.022 mmol) were dissolved in CH_2Cl_2 (1 mL). The yellow solution was stirred for 30 min. at room temperature, diphenylallyl acetate (140 μL) was added,

and the mixture was stirred for another 30 min and was then cooled to −20 °C. Dimethyl malonate (280 μL), *N*,*O*-bis(trimethyl)acetamide (BSA, 560 μL), and a few crystals of potassium acetate were added.[18] The mixture was stirred for 24 h at −20 °C, and was then hydrolyzed with water (NH_4Cl). The organic phase was filtered on silica gel. The enantiomeric excess was determined by HPLC on a DAICEL-OD-H column, hexanes/2-propanol = 99:1, L = 254 nm, t_R = 29.9 min (R), 32.5 min (S).

Computational section: All computed structures were fully optimized by use of GAUSSIAN 98.[28] For ONIOM[29] (B3LYP:[30]UFF[31]) computations, hydrogen atoms were used as linkers between the layers. The ONIOM partition is given in Scheme 5. All structures were analyzed by frequency computations, the imaginary frequencies correspond to C−N bond formation. For the smaller model systems, LanL2DZ-ECP basis sets[32] were augmented (+ d,p) with diffuse s-, p- (P, Pd) and d- (Pd) functions (addition of outermost function multiplied by 0.25) and polarization d-functions for P (exp. 0.34) and a f-function for Pd (exp. 1.472).[33]

Acknowledgement

We are grateful to the Fonds der Chemischen Industrie for financial support as well as for a Dozenten-Stipendium to B.G. We also thank the Deutsche Forschungsgemeinschaft (DFG) for support (GO-930/3-2, GO-930/5–1). We are grateful to Bayer AG, BASF AG, Wacker AG, Degussa AG, Raschig GmbH, Symrise GmbH, and OMG AG for generous gifts of laboratory equipment and chemicals. We also thank Prof. P. Hofmann for his support at Heidelberg.

[1] Recent reviews on total synthesis through palladium-catalyzed allylic substitutions: a) B. M. Trost, M. L. Crawley, *Chem. Rev.* **2003**, *103*, 2921; b) T. Graening, H.-G. Schmalz, *Angew. Chem.* **2003**, *115*, 2685; *Angew. Chem. Int. Ed.* **2003**, *42*, 2580.

[2] Reviews on catalyst design and mechanisms of palladium catalyzed allylic substitutions: a) B. M. Trost, C. Lee in *Catalytic Asymmetric Synthesis*, 2nd ed. (Ed.: I. Ojima), Wiley-VCH, New York **2000**, 593; b) G. Helmchen, *J. Organomet. Chem.* **1999**, *576*, 203; c) A. Pfaltz, M. Lautens in *Comprehensive Asymmetric Catalysis* (Eds.: E. N. Jacobsen, A. Pfaltz, H. Yamamoto), Springer, Heidelberg **1999**, p. 833; d) G. Helmchen, H. Steinhagen, S. Kudis in *Transition Metal Catalyzed Reactions* (Eds.: S.-I. Murahashi, S. G. Davies), Blackwell Science, Oxford **1999**, p. 241; e) B. M. Trost, D. L. Van Vranken, *Chem. Rev.* **1996**, *96*, 395.

[3] Side arm guidance of nucleophiles by hydroxylated phosphinoferrocenes: a) T. Hayashi, A. Yamamoto, T. Hagihara, Y. Ito, *Tetrahedron Lett.* **1986**, *27*, 191;b) T. Hayashi, K. Kanehira, T. Hagihara, M. Kumada, *J. Org. Chem.* **1988**, *53*, 113; c) T. Hayashi, *Pure Appl. Chem.* **1988**, *60*, 7; d) M. Sawamura, Y. Ito, *Chem. Rev.* **1992**, *92*, 857.

[4] Trost's C_2-symmetric diphosphane carboxamides based on 2-(diphenylphosphino)benzoic acid (dppba) and chiral diamines have large (≈110°) bite angles and furnish chiral pockets: a) B. M. Trost, X. Ariza, *J. Am. Chem. Soc.* **1999**, *121*, 10727;b) B. M. Trost, C. Heinemann, X. Ariza, S. Weigand, *J. Am. Chem. Soc.* **1999**, *121*, 8667; c) B. M. Trost, *Acc. Chem. Res.* **1996**, *29*, 566; d) B. M. Trost, B. Breit, S. Peukert, J. Zambrano, J. W. Ziller, *Angew. Chem.* **1995**, *107*, 2577; *Angew. Chem. Int. Ed. Engl.* **1995**, *34*, 2386.

[5] Electronic differentiation in P,N ligands has been most successfully applied in amino acid-based phosphinooxazoline (phox) ligands: a) G. Helmchen, S. Kudis, P. Sennhenn, H. Steinhagen, *Pure Appl. Chem.* **1997**, *69*, 513; b) G. Helmchen, A. Pfaltz, *Acc. Chem. Res.* **2000**, *33*, 336; c) J. Sprinz, G. Helmchen, *Tetrahedron Lett.* **1993**, *34*, 1769; c) P. von Matt, A. Pfaltz, *Angew. Chem.* **1993**, *105*, 614; *Angew. Chem. Int. Ed. Engl.* **1993**, *32*, 566.d) G. J. Dawson, C. G. Frost, J. M. J. Williams, S. J. Coote, *Tetrahedron Lett.* **1993**, *34*, 3149.

[6] a) H. Steinhagen, M. Reggelin, G. Helmchen, *Angew. Chem.* **1997**, *109*, 2199; *Angew. Chem. Int. Ed. Engl.* **1997**, *36*, 2108. The "*trans* phosphane preference" also explains memory effects in allylic substitutions: b) B. Goldfuss, U. Kazmaier, *Tetrahedron* **2000**, *56*, 6493. *trans*-effect in ferrocenyl ligands: c) T. Tu, Y.-G. Zhou, X.-L- Hou, L. X. Dai, X.-C. Dong, Y.-H. Yu, J. Sun, *Organometallics*, **2003**, *22*, 1255.

[7] Steric repulsion with equatorial P-phenyl groups: B. Wiese, G. Helmchen, *Tetrahedron Lett.* **1988**, *29*, 5727.

[8] a) M. Kollmar, H. Steinhagen, J. P. Janssen, B. Goldfuss, S. A. Malinovskaya, J. Vázquez, F. Rominger, G. Helmchen, *Chem. Eur. J.* **2002**, *8*, 3103; b) J. Vázquez, B. Goldfuss, G. Helmchen, *J. Organomet. Chem.* **2002**, *641* (1–2), 67; c) M. Kollmar, B. Goldfuss, M. Reggelin, F. Rominger, G. Helmchen, *Chem. Eur. J.* **2001**, *7*, 4913.

[9] For a recent review on chiral P,N ligands with pyridine units see: G. Chelicci, G. Orru, G. A. Pinna, *Tetrahedron* **2003**, *59*, 9471.

[10] Pyridyl phosphinites in allylic substitutions: F. Rahm, A. Fischer, C. Moberg, *Eur. J. Org. Chem.* **2003**, 4205.

[11] Camphor-derived P,N ligands for Ir catalysis: a) T. Bunlaksananusorn, K. Polborn, P. Knochel, *Angew. Chem.* **2003**, *115*, 4071; *Angew. Chem. Int. Ed.* **2003**, *42*, 3941; b) T. Bunlaksananusorn, A. P. Luna, M. Bonin, L. Micouin, P. Knochel, *Synlett* **2003**, *14*, 2240.

[12] Camphor and menthone derivatives: a) C. G. Arena, F. Nicolo, D. Drommi, G. Bruno, F. Faraone, *J. Chem. Soc. Chem. Commun.* **1994**, 2251; b) G. Chelucci, F. Socconlini, *Tetrahedron: Asymmetry* **1992**, *3*, 1235.

[13] Terpene-derived phosphinoquinolines: a) G. Chelucci, A. Saba, F. Soccolini, *Tetrahedron* **2001**, *57*, 9989; b) A. V. Malkov, M. Bella, G. Stara, P. Kocovsky, *Tetrahedron Lett.* **2001**, *42*, 3045.

[14] a) B. Goldfuss, T. Löschmann, F. Rominger, *Chem. Eur. J.* **2001**, *7*, 2028; b) B. Goldfuss, T. Löschmann, F. Rominger, *Chem. Eur. J.* **2001**, *7*, 2284.

[15] a) B. Goldfuss, F. Rominger, *Tetrahedron* **2000**, *56*, 881; b) B. Goldfuss, F. Eisenträger, *Aust. J. Chem.* **2000**, *53*, 53, 209.

[16] a) M. Steigelmann, Y. Nisar, F. Rominger, B. Goldfuss, *Chem. Eur. J.* **2002**, *8*, 5211; b) B. Goldfuss, M. Steigelmann, F. Rominger, *Eur. J. Org. Chem.* **2000**, 1785; c) B. Goldfuss, M. Steigelmann, *J. Mol. Model.* **2000**, *6*, 166; d) B. Goldfuss, M. Steigelmann, S. I. Khan, K. N. Houk, *J. Org. Chem.* **2000**, *65*, 77; e) B. Goldfuss, S. I. Khan, K. N. Houk, *Organometallics* **1999**, *18*, 2927.

[17] a) B. Goldfuss, "Enantioselective Addition of Organolithiums to C=O and Ethers" in *Topics in Organometallic Chemistry* (Ed.: D. M. Hodgson), Springer, Heidelberg **2003**; b) B. Goldfuss, M. Steigelmann, F. Rominger, H. Urtel, *Chem. Eur. J.* **2001**, *7*, 4456; c) B. Goldfuss, M. Steigelmann, F. Rominger, *Angew. Chem.* **2000**, *112*, 4299; *Angew. Chem. Int. Ed.* **2000**, *39*, 4133; Ref. [16e].

[18] The goal of this study is more the exploration and understanding of mechanisms leading to different enantioselectivities than the achievement of high enantioselectivities.

[19] Trost's BSA procedure: B. M. Trost, D. J. Murphy, *Organometallics* **1985**, *4*, 1143.

[20] H. Danjo, M. Higuchi, M. Yada, T. Imamoto, *Tetrahedron Lett.* **2004**, *45*, 603.

[21] a) P. Kocovsky, *J. Organomet. Chem.* **2003**, *687*, 256; b) J. Yin, M. P. Rainka, X.-X. Zhang, S. L. Buchwald, *J. Am. Chem. Soc.* **2002**, *124*, 1162; c) G. C. Lloyd-Jones, S. C. Stephen, M. Murray, C. P. Butts, S. Vyskocil, P. Kocovsky, *Chem. Eur. J.* **2000**, *6*, 4348; d) T. Hayashi, *Acc. Chem. Res.* **2000**, *33*, 354; e) P. Kocovsky, S. Vyskocil, I. Cisarova, J. Sejbal, I. Tislerova, M. Smrcina, G. C. Lloyd-Jones, S. C. Stephen, C. P. Butts, M. Murray, V. Langer, *J. Am. Chem. Soc.* **1999**, *121*, 7714. High branch selectivity was found for MOP in allylic substitutions: f) T. Hayashi, M. Kawatsura, Y. Uozumi, *Chem. Commun.* **1997**, 561.

[22] B. M. Trost, F. D. Toste, *J. Am. Chem. Soc.* **1999**, *121*, 4545.

[23] a) H. Hagelin, B. Akermark, P.-O. Norrby, *Chem. Eur. J.* **1999**, *5*, 902. In a H_3N-allyl-Pd$(NH_3)_2$ transition structure, the H_3N-C(allyl)-Pd distances were computed (B3LYP/LanL2DZ) to be 1.96 Å and 2.85 Å. Previous computations on Pd-catalyzed allylic substitutions: b) P. E. Blöchl, A. Togni, *Organometallics* **1996**, *15*, 4125; c) T. R. Ward, *Organometallics* **1996**, *15*, 2836.

[24] The absolute configuration of the substitution products (*R* vs. *S*) is chosen to corresponds to the experimental nucleophile malonate. For consistency, the CIP priority sequence is maintained as Ph > Nu > vinyl > H for both experimental (Nu = malonate) and computational (Nu = NH_3) nucleophiles.

[25] G. S. Hammond, *J. Am. Chem. Soc.* **1955**, *77*, 334.

[26] a) V. Lecomte, E. Stephan, G. Jaouen, *Tetrahedron Lett.* **2002**, *43*, 3463; b) R. Pallaud, J. Pleau, *C. R. Seances Acad. Sci. Ser. C* **1967**, 265, 1479.

[27] a) W. A. Herrmann, J. J. Haider, J. Fridgen, G. M. Lobmaier, M. Spiegler, *J. Organomet. Chem.* **2000**, *603*, 69; b) M. Genov, K. Kostova, V. Dimitrov, *Tetrahedron: Asymmetry* **1997**, *8*, 1869.

[28] Gaussian 98, Revision A.9, M. J. Frisch, G. W. Trucks, H. B. Schlegel, G. E. Scuseria, M. A. Robb, J. R. Cheeseman, V. G. Zakrzewski, J. A. Montgomery, Jr., R. E. Stratmann, J. C. Burant, S. Dapprich, J. M. Millam, A. D. Daniels, K. N. Kudin, M. C. Strain, O. Farkas, J. Tomasi, V. Barone, M. Cossi, R. Cammi, B. Mennucci, C. Pomelli, C. Adamo, S. Clifford, J. Ochterski, G. A. Petersson, P. Y. Ayala, Q. Cui, K. Morokuma, D. K. Malick, A. D. Rabuck, K. Raghavachari, J. B. Foresman, J. Cioslowski, J. V. Ortiz, A. G. Baboul, B. B. Stefanov, G. Liu, A. Liashenko, P. Piskorz, I. Komaromi, R. Gomperts, R. L. Martin, D. J. Fox, T. Keith, M. A. Al-Laham, C. Y. Peng, A. Nanayakkara, M. Challacombe, P. M. W. Gill, B. Johnson, W. Chen, M. W. Wong, J. L. Andres, C. Gonzalez, M. Head-Gordon, E. S. Replogle, J. A. Pople, Gaussian, Inc., Pittsburgh PA, **1998**.

[29] a) S. Dapprich, I. Komaromi, K. S. Byun, K. Morokuma, M. J. Frisch, *J. Mol. Struct.* **1999**, *461–462*, 1; b) M. Svensson, S. Humbel, R. D. J. Froese, T. Matsubara, S. Sieber, K. Morokuma, *J. Phys. Chem.* **1996**, *100*, 19357; c) S. Dapprich and T. Vreven, personal communications on ONIOM implementations in G98 with B.G.

[30] a) A. D. Becke, *J. Chem. Phys.* **1993**, *98*, 5648; b) C. Lee, W. Yang, R. G. Parr, *Phys. Rev. B* **1988**, *37*, 785; c) Implementation in G98: P. J. Stephens, F. J. Devlin, C. F. Chabalowski, M. J. Frisch, *J. Phys. Chem.* **1994**, *98*, 11623.

[31] A. K. Rappé, C. J. Casewit, K. S. Colwell, W. A. Goddard, III, W. M. Skiff, *J. Am. Chem. Soc.* **1992**, *114*, 10024.

[32] P. J. Hay, W. R. Wadt, *J. Chem. Phys.* **1985**, *82*, 270.

[33] a) A. W. Ehlers, M. Böhme, S. Dapprich, A. Gobbi, A. Höllwarth, V. Jonas, K. F. Köhler, R. Stegmann, A. Veldkamp, G. Frenking, *Chem. Phys. Lett.* **1993**, *208*, 111; b) *Gaussian Basis Sets for Molecular Calculations*, (Ed.: S. Huzinaga), Elsevier, Amsterdam, **1984**.

Received: March 20, 2004
Published online: September 20, 2004

